Spectroscopic, electrochemical and computational studies of rhenium(I) and ruthenium(II) complexes incorporating the novel tetradentate ligand 1,4-bis(4-(4′-methyl)-2,2′-bipyridyl)-2,3-diaza-1,3-butadiene (BBDB) and its derivatives

Mauricio Cattaneo [a], Mónica M. Vergara [a], Mónica E. García Posse [a], Florencia Fagalde [a], Teodor Parella [b], Néstor E. Katz [a],*

[a] INQUINOA-CONICET, Instituto de Química Física, Facultad de Bioquímica, Química y Farmacia, Universidad Nacional de Tucumán, Ayacucho 471, T4000INI San Miguel de Tucumán, Argentina
[b] Servei de RMN, Universitat Autònoma de Barcelona, Bellaterra, 08193 Barcelona, Spain

ARTICLE INFO

ABSTRACT

The novel tetradentate ligand 1,4-bis(4-(4′-methyl)-2,2′-bipyridyl)-2,3-diaza-1,3-butadiene (BBDB) was synthesized and characterized by spectroscopic techniques. New complexes of Re and Ru of formulae: [Re(BBDB)(CO)$_3$(Cl)], [(CH$_3$CN)(CO)$_3$Re(μ-BBDB)Re–(CO)$_3$(CH$_3$CN)]$^{2+}$, [(bpy)$_2$Ru-(μ-BBDB)Ru(bpy)$_2$]$^{4+}$, [(NH$_3$)$_4$Ru(μ-BBDB)–Ru(NH$_3$)$_4$]$^{4+}$ (bpy = 2,2′-bipyridine) and complexes of Ru with 4-Me-4′-CO$_2$H-bpy (=4-methyl-4′-carboxylic acid-2,2′-bipyridine) – the hydrolyzed derivative of BBDB – of formulae: [(Ru(4-Me-4′-CO$_2$H-bpy)(bpy)$_2$]$^{2+}$ and [Ru(4-Me-4′-CO$_2$H-bpy)(CN)$_4$]$^{2-}$ were prepared and characterized by spectroscopic, electrochemical and computational techniques. The disclosed enhanced electronic coupling in the mixed-valent complex with ruthenium ammines can be explained by the electronic delocalization imposed by the —C=N—N=C— backbone. DFT and TD-DFT calculations can predict the optical properties and electronic structures of the reported complexes and comparisons with calculations performed on previously reported complexes with 4-pyridinaldazine can account for their photophysical behaviour.

© 2013 Elsevier Ltd. All rights reserved.

1. Introduction

Polypyridines have been extensively used as versatile ligands capable of octahedral coordination around transition metal centers. Moreover, those polypyridyl ligands that connect two or more metal centers especially derivatives of 2,2′-bipyridine are the basis in building antenna complexes, one-, two-, or tridimensional solids and systems relevant to energy conversion schemes [1,2].

Bridging polypyridines are excellent ligands for testing long-distance transmission of electronic interactions in dinuclear symmetric and asymmetric mixed-valent complexes [3–6]. The distance dependence of electronic transmission between two metallic centers is an important issue in connection to electron and energy transfer processes [7,8].

We have already reported the syntheses and spectroscopic, electrochemical and photophysical properties of a series of coordination compounds with the bridging ligand 4-PCA

(4-pyridinecarboxaldheydeazine or 4-pyridinealdazine or 1,4-bis(4-pyridyl)-2,3-diaza-1,3-butadiene) whose structure is shown in Scheme 1. An enhancement of the electronic coupling was disclosed when comparing the inter-metallic electronic coupling in mixed-valent species containing 4-PCA with related complexes with similar metal-metal distances containing aromatic bridging ligands [9]. Other complexes containing 4-PCA have been studied as models for building luminescent molecular sensors [10,11].

In this work, in order to increase the stability and rigidity of a bridging azine such as 4-PCA, we have attempted to synthesize and characterize the novel ligand 1,4-bis(4-(4′-methyl)-2,2′-bipyridyl)-2,3-diaza-1,3-butadiene (BBDB) whose structure is shown in Scheme 2. This ligand has the same —C=N—N=C— linkage as 4-PCA. We also report the synthesis, spectroscopic and electrochemical characterization of some new mononuclear and dinuclear complexes incorporating BBDB and one of its hydrolyzed derivatives with the well-known tricarbonylrhenium(I), bis(2,2′-bipyridine)ruthenium(II) and tetraammineruthenium(II) moieties. Experimental results are compared with computational analysis using DFT and TD-DFT methods and also compared with previous studies with the related bridging ligand 4-PCA [10].

* Corresponding author.
E-mail addresses: teodor.parella@uab.es (T. Parella), nkatz@fbqf.unt.edu.ar (N.E. Katz).
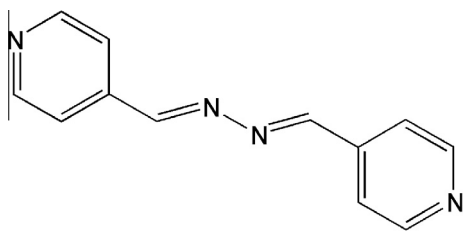
Scheme 1. Structure of 4-PCA.
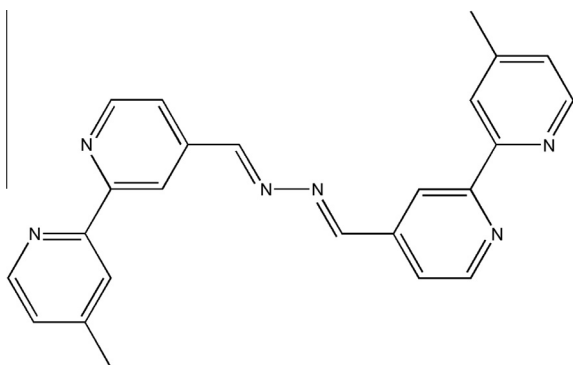
Scheme 2. Structure of BBDB.

Tricarbonylpolypyridylrhenium(I) complexes of the type $[Re(diimine)(CO)_3(L)]^{n+}$ present a rich manifold of ground- and excited-states physicochemical properties. The possibility of structural variations of the diimine and/or the axial ligand L have led to applications of these complexes as sensors [12], molecular switches [13], probes for cell imaging [14], photochromism [15], CO_2 reduction [16], and so on. On the other hand, polypyridylruthenium(II), amineruthenium(II) and cyanoruthenium(II) complexes are of considerable interest due to their spectroscopic, electrochemical, photophysical and reactivity properties which have led to applications in artificial photosynthesis [17]; besides, they are useful models for energy and/or electron transfer processes [18,19].

2. Experimental

2.1. Materials and methods

All used chemicals were p.a. grade. CH_3CN was freshly distilled over P_4O_{10} for electrochemical measurements. Tetrakis(*n*-butyl)ammonium hexafluorophosphate (TBAH) was recrystallized four times from EtOH and dried at 150 °C for 72 hs. Chemical analyses were performed at INQUIMAE (University of Buenos Aires, Argentina), with an estimated error of ±0.5%. IR spectra were performed as KBr pellets on a FTIR Perkin-Elmer Spectrum RX-I spectrophotometer. UV–Vis spectra were recorded with a Varian Cary 50 spectrophotometer in 1-cm cells. Emission spectra were obtained with a Shimadzu RF-5301 PC spectrofluorometer at room temperature. A Dewar cooled finger system was used to obtain spectra in MeOH/EtOH 4:1 matrix at 77 K. Cyclic voltammetry experiments were carried out in CH_3CN (0.1 M TBAH) with a BAS Epsilon EC equipment. A standard three-electrode cell was used with Ag/AgCl (3 M KCl) as a reference electrode, vitreous C as a working electrode and Pt wire as an auxiliary electrode. NMR spectra were recorded in CD_3CN with Bruker Avance 500 and 200 MHz spectrometers.

2.2. Preparation of BBDB

This ligand was synthesized from 4-methyl-4′-formyl-2,2′-bipyridine (4-Me-4′-COH-bpy), prepared as reported by Strouse et al. [20]. 1 eq of hydrazine hydrate dissolved in EtOH was added slowly during 30 min, under continuous stirring, to a solution of 2 eq of 4-Me-4′-COH-bpy in EtOH. The yellow mixture was stirred for 8 h and a precipitate appeared overnight. The bright yellow needles were filtered and washed with EtOH and ether. The obtained solid was scarcely soluble in almost all solvents, except $CHCl_3$ and CH_2Cl_2. Yield: 325 mg (83%). *Anal.* Calc. for $C_{24}H_{20}N_6$ (392.46): C, 73.4; H, 5.1; N, 21.4. Found: C, 73.0; H, 5.0; N, 21.0%. IR (KBr): 3055 (w), 3014 (w), 2956 (w), 2918 (w), 2856 (w), 1635 (m), 1594 (s), 1552 (s), 1458 (m), 1432 (m), 1371 (s), 1327 (m), 1277 (w), 1218 (w), 1156 (w), 1106 (w), 1066 (w), 988 (w), 970 (w), 903 (w), 826 (s), 748 (w), 684 (m), 669 (w), 530 (m), 414 (w) cm^{-1}. ^1H NMR (200 MHz, $CDCl_3$, 25 °C): δ = 8.81 (d, 2H J_{9-10} = 5 Hz), 8.76 (d, 2H J_{7-9} = 1 Hz), 8.70 (s, 2H), 8.60 (d, 2H J_{1-2} = 5 Hz), 8.28 (d, 2H J_{2-4} = 1 Hz), 7.82 (dd, 2H J_{9-10} = 5 Hz, J_{7-9} = 1 Hz), 7.19 (dd, 2H J_{1-2} = 5 Hz, J_{2-4} = 1 Hz), 2.47 (s, 6H). ^{13}C NMR (200 MHz, $CDCl_3$, 25 °C): δ = 160.67, 157.4, 155.26, 149.77, 149.12, 148.30, 141.86, 125.11, 122.08, 121.31, 120.66, 21.22.

2.3. Preparation of [Re(BBDB)(CO)₃Cl]·0.5CH₃COCH₃ (1)

This complex was synthesized according to procedures similar to those already reported [21]. $Re(CO)_5Cl$ (70 mg, 0.19 mmol) dissolved in 10 mL of methanol was added by dropping to a suspension of BBDB (392 mg, 1 mmol) in chloroform and then the mixture was refluxed under stirring for 3 h. After cooling, the suspension was filtrated to remove the insolubles and it was washed three times with CH_3CN. The filtrate was roto-evaporated to dryness, re-suspended in CH_3CN and filtrated. The resulting solid was dissolved in acetone, precipitated with ether, filtrated and dried under vacuum over P_4O_{10}. Yield: 43 mg (31%). *Anal.* Calc. for $C_{28.5}H_{23}ClN_6O_{3.5}Re$ (727.19): C, 47.1; H, 3.2; N, 11.6. Found: C, 47.2; H, 3.3; N, 11.8%. IR (KBr): $\nu(CO)$ = 2020, 1912, 1894 cm^{-1}.

2.4. Preparation of [Cl(CO)₃(Re)(μ-BBDB)Re(CO)₃Cl]·0.5CH₂Cl₂ (2)

This species was prepared by following the technique of Baiano et al. [22]. BBDB (59 mg, 0.15 mmol) was dissolved in 40 mL of dichloromethane. Then, $Re(CO)_5Cl$ (109 mg, 0.30 mmol) dissolved in 30 ml of methanol was added and the mixture was refluxed for 4 h. The reddish precipitate was filtrated and washed with dichloromethane and methanol. Yield: 52 mg (33%). *Anal.* Calc. for $C_{30.5}H_{21}Cl_3N_6O_6Re_2$ (1046.31): C, 35.0; H, 2.0; N, 8.0. Found: C, 35.2; H, 2.3; N, 8.5%. IR (KBr): ν (CO) = 2022, 1918, 1892 cm^{-1}. NMR spectra could not be obtained due to the insolubility of this complex.

2.5. Preparation of [(CH₃CN)(CO)₃Re(μ-BBDB)Re(CO)₃(CH₃CN)](TFMS)₂·4H₂O (3)

This complex was prepared by heating $[Cl(CO)_3Re(\mu$-BBDB)Re(CO)_3Cl]$ (50 mg, 0.05 mmol) with AgTFMS (30 mg, 0.0117 mmol) under reflux in CH_3CN during 1 h. The insoluble reddish precipitate disappeared while the solution turned orange-yellow. After cooling, AgCl was filtrated and the filtrate evaporated to dryness, re-suspended in acetone, precipitated with ether, filtrated and washed with ether. Yield: 25 mg (36%). *Anal.* Calc. for $C_{36}H_{34}F_6N_8O_{16}Re_2S_2$ (1385.24): C, 31.2; H, 2.4; N, 8.1; S, 4.6. Found: C, 31.3; H, 1.9; N, 8.2; S, 4.2%. IR (KBr): $\nu(CO)$ = 2038, 1924 cm^{-1}. ^1H NMR (500 MHz, CD_3CN) δ = 9.15 (d, 2H J = 5.8 Hz), 8.89 (d, 2H J_{7-9} = 5.6 Hz), 8.89 (s, 2H), 8,72 (s, 2H), 8.51 (s, 2H), 8.11 (dd, 2H J = 5.8 Hz, J = 1.2 Hz), 7.60 (d, 2H J = 5.6 Hz), 2.63 (s,

6H). ^{13}C NMR (200 MHz, CDCl$_3$) δ = 194.8, 194.7, 191.4, 158.3, 158.2, 156.1, 155.6, 155.0, 154.3, 145.75, 130.1, 126.6, 126.4, 123.6, 21.6.

2.6. Preparation of [(bpy)$_2$Ru(μ-BBDB)Ru(bpy)$_2$](PF$_6$)$_4$ (**4**)

This complex was synthesized according to previous protocols [23]. cis-[Ru(bpy)$_2$Cl$_2$]·2H$_2$O (250 mg, 0.48 mmol) was mixed with BBDB (377 mg, 0.96 mmol) in 50 mL of methanol and refluxed under stirring in the darkness during 5 h. The dark purple solution turned reddish-orange and the white unreacted ligand remained. This solid was filtrated and the filtrate was evaporated to dryness and re-suspended in 10 mL of H$_2$O. A solution of 2 g of NH$_4$PF$_6$ in 10 mL of H$_2$O was then added to induce precipitation. The solid was chromatographied in alumina with toluene/acetonitrile as a mobile phase and then rotoevaporated to complete dryness. Yield: 162 mg (38%). *Anal.* Calc. for C$_{64}$H$_{52}$N$_{14}$F$_{24}$Ru$_2$P$_4$ (1799.21): C, 42.7; H, 2.9; N, 10.9. Found: C, 42.9; H, 3.2; N, 10.6%. IR (KBr): 1622, 1465, 1447, 1424, 1313, 1236, 842, 764, 732, 558 cm^{-1}. ^{1}H NMR (200 MHz, CD$_3$CN) δ = 8.72 (s, 2H), 8.57 (s, 4H), 8.53 (m, 8H), 8.15–8.04 (m, 12H), 7.82–7.74 (m, 6H), 7.62 (d, 2H, J = 6 Hz), 7.48–7.40 (m, 10H), 7.34 (d, 2H, J = 5,8 Hz), 2.60 (s, 6H). ^{13}C NMR (200 MHz, CD$_3$CN) δ = 157, 153–151, 151, 138–137, 129, 128–127, 125–123, 20.

2.7. Preparation of [(NH$_3$)$_4$Ru(μ-BBDB)Ru(NH$_3$)$_4$](PF$_6$)$_4$ (**5**)

This complex was synthesized by procedures similar to those already reported [24–26]. A solution of BBDB (19.8 mg, 0.05 mmol) in 10 mL of acetone was mixed with a solution of [Ru(NH$_3$)$_5$(H$_2$-O)](PF$_6$)$_2$ (50 mg, 0.10 mmol) prepared as described before [27], in 10 mL of acetone under Ar bubbling for 1hr. The solution turned dark blue and it was precipitated with 100 mL of CHCl$_3$ and 50 ml of ether. Then it was filtrated, washed with ether and dried under vacuum. The solid was chromatographied in alumina with CH$_3$CN/MeOH 4:1 as mobile phase and the dark blue band collected, rotoevaporated and recrystallized from acetone/ether. Yield: 17 mg (26%). *Anal.* Calc. for C$_{24}$H$_{44}$N$_{14}$Ru$_2$F$_{24}$P$_4$ (1310.7): C, 22.0; H, 3.4; N, 15.0. Found: C, 21.9; H, 3.4; N, 15.0%. IR (KBr): 3228 (m), 3171 (m), 1618 (m), 1400 (m), 1274 (m), 1014 (w), 834 (s), 560 (s) cm^{-1}. ^{1}H NMR (200 MHz, CD$_3$CN): δ = 9.15 (2H, d, J_{1-2} = 6.1 Hz), 7.84 (2H, dd, J_{2-4} = 1.2 Hz), 8.62 (2H, d), 8.75 (2H, d, J_{7-8} = 5.9 Hz), 7.40 (2H, dd, J_{8-10} = 0.7 Hz), 8.30 (2H, d), 8.80 (2H, s), 1.51 (6H, s), 1.86 (6H, s), 2.30 (6H, s), 2.99 (6H, s). ^{13}C NMR (200 MHz, CD$_3$CN): δ = 155.2, 123.0, 138.2, 121.6, 163.5, 153.6, 127.3, 147.7, 124.6, 161.1, 160.4, 20.9.

2.8. Preparation of [Ru(bpy)$_2$(4-Me-4′-CO$_2$H-bpy)](PF$_6$)$_2$ (**6**)

This complex was obtained as a by-product of the synthesis of complex (**5**). When performing the chromatography using Sephadex G-25 and water as a mobile phase, the BBDB bridging ligand was hydrolyzed to 4-Me-4′-CO$_2$H-bpy. Crystals from a slow evaporation from water were obtained. Yield: 27 mg (60%). *Anal.* Calc. for C$_{32}$H$_{26}$N$_6$O$_2$RuF$_{12}$P$_2$ (917.6): C, 41.9; H, 2.9; N, 9.2. Found: C, 41.5; H, 3.3; N, 9.8%. IR (KBr): 1709, 1619, 1606, 1465, 1447, 1424, 1313, 1236, 842, 764, 732, 558 cm^{-1}. ^{1}H NMR (200 MHz, CD$_3$CN): δ = 8,95 (s, 1H), 8.54 (s, 1H), 8.52(m, 4H), 8.08 (m, 4H), 7.80 (s, 2H), 7.75 (m, 4H), 7.57 (d, 1H, J = 5.5 Hz), 7.42 (m, 4H), 7.27 (d, 1H), 3.61 (broad-acid, 1H), 2.25 (s, 3H). ^{13}C NMR (200 MHz, CD$_3$CN): δ = 167.3, 158.9, 157.5, 152.9, 152.8, 151.9, 145.4, 138.8, 129.7, 128.7, 127.8, 126.6, 125.4, 124.5, 21.2. This complex has already been reported [28].

2.9. Preparation of K$_2$[Ru(4-Me-4′-CO$_2$H-bpy)(CN)$_4$]·4H$_2$O (**7**)

This species was synthesized according to procedures reported by Herrera *et al.* [29]. K$_4$[Ru(CN)$_6$]·3H$_2$O (178 mg, 0.38 mmol) dissolved in water acidulated with HCl (pH 1.3) was mixed with BBDB (150 mg, 0.38 mmol) in MeOH (ratio v:v 3:1) and refluxed with stirring during 24 h. The red-brick solution was cooled down to room temperature and filtrated to remove excess BBDB. The solution was neutralized with KOH 0.1 M, and reduced to a minimum volume. Ethanol was added to remove excess K$_4$[Ru(CN)$_6$]. The resulting solution was evaporated to dryness, re-dissolved in the minimum volume of water and chromatographied on Sephadex G-25 eluting with water. An orange powder was obtained. As described in the case of complex (**6**), BBDB was hydrolyzed to 4-Me-4′-CO$_2$H-bpy. Yield: 43 mg (20%). *Anal.* Calc. for K$_2$C$_{16}$H$_{18}$N$_6$O$_6$Ru (569.72): C, 33.7; H, 3.2; N, 14.7. Found: C, 33.8; H, 3.3; N, 14.7.

2.10. Computational procedures

All calculations were carried out with Gaussian-03 program package [30]. Electronic structure of the ground states of all species were optimized by using DFT (Density Functional Theory) calculations. The Perdew, Burke, Ernzerhof exchange and correlation functionals (PBE1PBE) [31,32] were used with the LANL2DZ basis set for Re and 6-311G(d) for H, C, O and N. For Ru complexes calculations were carried out with the LANL2DZ basis set which uses Dunning D95V basis set on C, N, O, H and Los Alamos ECP plus DZ on Ru. The vertical transition energies were calculated at the optimized ground-state geometries in vacuum for the lowest 60 singlet to singlet excitation energies using time-dependent density functional theory (TD-DFT) with hybrid PBE1PBE functionals, LANL2DZ basis set for Re and 6-311+G(d) for H, C, O and N and including a dielectric medium as an approximation to include solvent polarization effects. The inclusion of the dielectric medium was calculated using the CPCM reaction field model with acetonitrile as solvent. The geometries of the lowest excited triplet states (T1) were calculated by using un-restricted B3LYP method with LANL2DZ basis set and CPCM model with acetonitrile as solvent. Mulliken population analysis, partial density of states (PDOS) calculations and simulated electronic spectra were determined by using the GAUSSSUM 2.2 program, with a half-width of 3000 cm^{-1} for Ru complexes and 5000 cm^{-1} for Re complexes [33].

3. Results and discussion

3.1. Syntheses

The novel ligand 1,4-bis(4-(4′-methyl)-2,2′-bipyridyl)-2,3-diaza-1,3-butadiene (BBDB) was obtained by a Schiff base condensation reaction of an aldehyde with hydrazine [10]. It has the capacity to coordinate two metallic centers through the two bipyridyl units and it is similar to other bridging ligands derived from 2,2′-bpy [20,21], but has the peculiarity of having a 2,3-diaza-1,3-butadiene (—C═N—N═C—) linker. BBDB was thoroughly characterized by chemical analysis, IR, UV–Vis and NMR spectra. However, its low solubility in almost any solvent prevented the measurement of electrochemical properties and the synthesis of mononuclear complexes.

Several new complexes of Re and Ru incorporating BBDB were synthesized when organic solvents were used. In most cases, the primary products were the symmetric dinuclear complexes. Several attempts were done to prepare the corresponding mononuclear complexes, but no pure compounds could be obtained. When water was used in the synthetic or in the purification

procedures, BBDB was hydrolyzed to 4-Me-4′-CO$_2$H-bpy (=4-methyl-4′-carboxylic acid-2,2′-bipyridine); its structure is shown in Scheme 3. Almost all the new complexes were soluble in acetonitrile; their purity was confirmed by chemical analyses, IR and NMR spectra. As expected for complexes with ligands containing the —C≡N—N≡C— backbone [9], a zigzag trans-structure is preferred for BBDB and its complexes and no evidence for cis–trans linkage isomerization processes was obtained.

3.2. UV–Vis spectra

Table 1 shows the electronic spectral data for BBDB and its complexes. The UV/Vis spectrum of BBDB shows strong absorptions at λ_{max} = 284 and 251 nm, with shoulders between 310 and 320 nm, in CH$_2$Cl$_2$. The wavenumber of the lowest energy transition is very similar to that reported for the ligand 4-PCA [9]. The band at λ_{max} = 251 nm is due to bpy's π–π* transitions. A more detailed discussion about the electronic states involved will be shown below in the computational studies section.

Rhenium(I) complexes display UV–Vis spectra similar to those of related tricarbonyl(polypyridyl)rhenium(I) complexes: the lowest energy band between 400 and 350 nm can be assigned to MLLCT (metal–ligand-to-ligand charge transfer) (CO)$_3$d$_\pi$ (Re) → π*(BBDB) transitions, while those below 350 nm can be attributed to intraligand π–π* transitions. For example, the mononuclear species [Re(BBDB)(CO)$_3$Cl], (**1**), has the MLLCT band at λ_{max} = 382 nm which can be compared to the value corresponding to the complex [Re(Ph$_2$bpy)(CO)$_3$Cl] (λ_{max} = 384 nm) [34] that has two conjugated phenyl groups in the 4,4′-positions of the pyridyl rings. This similarity is consistent with the electron accepting properties of the —C≡N—N≡C— backbone. [Cl(CO)$_3$Re(μ-BBDB)Re(CO)$_3$Cl], (**2**), was insoluble in all the used solvents and could not be characterized by UV–Vis spectroscopy. Fig. 1 shows the UV–Vis spectrum of the dinuclear ion [(CH$_3$CN)(CO)$_3$Re(μ-BBDB)Re(CO)$_3$(CH$_3$CN)]$^{2+}$, cation of (**3**): its lowest energy absorption band appears at λ_{max} ~ 374 nm, as expected when replacing an electron donor ligand (Cl) by an electron accepting one (CH$_3$CN) in the Re coordination sphere.

The dinuclear complex [(bpy)$_2$Ru(μ-BBDB)Ru(bpy)$_2$]$^{4+}$, cation of (**4**), has a spectral pattern similar to that of [Ru(bpy)$_3$]$^{2+}$, as shown in Fig. 2, with its lowest energy band at λ_{max} = 458 nm which is readily assigned to combined d$_\pi$(Ru) → π*(bpy) and d$_\pi$(Ru) → π* (BBDB) MLCT (metal-to-ligand charge transfer) transitions [1]. The intense band at λ_{max} = 288 nm can be assigned to mixed π → π*(bpy) and π → π*(BBDB) transitions.

The dinuclear complex [(NH$_3$)$_4$Ru(μ-BBDB)Ru(NH$_3$)$_4$]$^{4+}$, cation of (**5**), has a spectrum with a lower energy transition at λ_{max} = 568 nm, assigned to d$_\pi$(Ru) → π*(BBDB) MLCT transition and higher energy transitions at λ_{max} = 308 and 275 nm, assigned to π → π*(BBDB) transitions. Spectrophotometric titration with Br$_2$ in CH$_3$CN caused complete disappearance of the band at λ_{max} = 568 nm, as shown in Fig. 3. This oxidation was reversible, since the original complex could be almost completely recovered when adding SnCl$_2$ as a reductant (Fig. 3). However, the mixed-valent species [(NH$_3$)$_4$Ru(μ-BBDB)Ru(NH$_3$)$_4$]$^{5+}$ did not show IVET

transitions in the near-IR region, as it was the case for the related complex [(NH$_3$)$_5$Ru(μ-4-PCA)Ru(NH$_3$)$_5$]$^{5+}$ [9], which could be due to a very low extinction coefficient.

The mononuclear complex with the hydrolyzed ligand derived from BBDB, of formula [(Ru(4-Me-4′-CO$_2$H-bpy)(bpy)$_2$]$^{2+}$, cation of (**6**), has typical absorptions expected for ruthenium bypyridyls [1]. The other complex with the same ligand of formula [Ru (4-Me-4′-CO$_2$H-bpy)(CN)$_4$]$^{2-}$, anion of (**7**), has MLCT bands similar to those of tetracyanoruthenium(II) species with bypyridyl derivatives [35].

3.3. IR Spectra

The IR spectrum of BBDB shows the C≡N stretching band at v = 1635 cm^{-1}, a typical value for Schiff bases. For rhenium complexes with Cl$^-$ ligands in the coordination sphere, three bands were observed in the region corresponding to the carbonyl stretching frequencies, v(C≡O) = 2020, 1912 and 1894 cm^{-1} for (**1**) and 2022, 1918 and 1892 cm^{-1} for (**2**). This result is consistent with a facial configuration of carbonyl groups bonded to Re (with local C_{3v} symmetry) and a σ donor ligand in the sixth position [34]. However, for complex (**3**) of formula [(CH$_3$CN)(CO)$_3$Re(μ-BBDB)Re(CO)$_3$(CH$_3$CN)](TFMS)$_2$·4H$_2$O higher values of v(C≡O) are observed (2038 cm^{-1} and 1924 cm^{-1}) reflecting the change of the axial ligand from a σ-donor (Cl$^-$) to a π-acceptor goup (CH$_3$CN). Absorption between 1630 and 1600 cm^{-1}, typical of C≡N stretching vibrations, is detectable in all complexes. The bipyridylruthenium(II) dinuclear complex (**4**) of formula [(bpy)$_2$Ru(μ-BBDB)Ru(bpy)$_2$](PF$_6$)$_4$ shows an IR spectrum with characteristic bpy bands. The IR spectrum of the tetraammineruthenium(II) dinuclear complex (**5**) of formula [(NH$_3$)$_4$Ru(μ-BBDB)Ru(NH$_3$)$_4$](PF$_6$)$_4$ displays broad and structured bands between 3300 and 3100 cm^{-1}, assigned to N–H stretchings and a band at 1276 cm^{-1}, assigned to the symmetric ammonia deformation δ_{sym}(NH$_3$); the observed values are consistent with oxidation state (II) for Ru [9]. Finally, the mononuclear species (**6**) of formula [Ru(4-Me-4′-CO$_2$H-bpy)(bpy)$_2$](PF$_6$)$_2$ shows distinguishing bpy bands while the mononuclear complex (**7**), of formula K$_2$[Ru(4-Me-4′-CO$_2$H-bpy)(CN)$_4$]·4H$_2$O shows v(C≡N) stretching bands centered at 2058 cm^{-1} which is typical of tetracyanorutenate groups [35].

3.4. NMR spectra

All ^{1}H and ^{13}C NMR data for BBDB and its complexes are shown in the Experimental Section. Complete resolution of the signals could be accomplished by using bidimensional techniques, such as COSY, ^{13}C HSQC and ^{13}C HMBC.

Thus, NMR experiments in CDCl$_3$ allowed a complete characterization of BBDB; its C_i symmetry was disclosed by the appearance of a set of 8 signals in the ^{1}H NMR spectrum and a set of 12 signals in the ^{13}C NMR spectrum. The complete assignments of all H and C atoms are shown in Scheme 4.

The same set of signals are expected in the ^{1}H NMR spectra of dinuclear symmetric BBDB complexes. Fig. 4 shows the ^{1}H NMR spectra of BBDB and complexes (**3**) and (**5**) between 7 and 9 ppm for comparison purposes. The set of 7 signals corresponding to the aromatic protons show the influence of the metal centers over H2, H9 and H14 (see Scheme 4 for proton numbering). In contrast, due to symmetry loss a set of 16 signals corresponding to BBDB are expected in the ^{1}H NMR spectra of mononuclear Re or Ru complexes of this ligand.

3.5. Electrochemical properties

Table 2 shows the anodic and cathodic peak potentials (E_{pa} and E_{pc} respectively) of all complexes, as determined by CV in CH$_3$CN
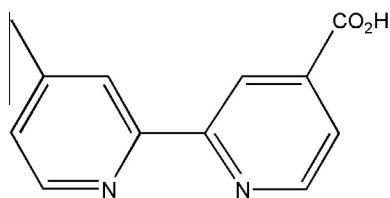
Scheme 3. Structure of 4-Me-4′-CO$_2$H-bpy.

Table 1
Electronic absorption spectral data, in CH_3CN, at 22 °C.

Compound	λ_{max} [nm] ($10^{-3}\varepsilon_{max}$ [M^{-1} cm^{-1}])
BBDB[a]	284 (40.5), 251 (27.8)
[Re(BBDB)(CO)$_3$(Cl)], (**1**)	382 (6.2), 288 (30.9), 245 (26.5)
[(CH$_3$CN)(CO)$_3$Re(μ-BBDB)Re(CO)$_3$(CH$_3$CN)]$^{2+}$, cation of (**3**)	374 (18.3), 284 (39.9), 254 (39.5)
[(bpy)$_2$Ru(μ-BBDB)Ru(bpy)$_2$]$^{4+}$, cation of (**4**)	458 (21.7), 438 (sh), 288 (103.4), 245 (38.4)
[(NH$_3$)$_4$Ru(μ-BBDB)Ru(NH$_3$)$_4$]$^{4+}$, cation of (**5**)	720 (sh), 568 (12.2), 480 (8.7), 369 (7.0), 308 (26.8), 275(25.7)
[(Ru(4-Me-4′-CO$_2$H-bpy)(bpy)$_2$]$^{2+}$, cation of (**6**)	455 (11.4), 433 (sh), 287 (62.5), 244 (23.4)
[Ru (4-Me-4′-CO$_2$H-bpy)(CN)$_4$]$^{2-,b}$, anion of (**7**)	416 (5.1), 289 (22.5), 240(16.2)

[a] In CH_2Cl_2.
[b] In H_2O.
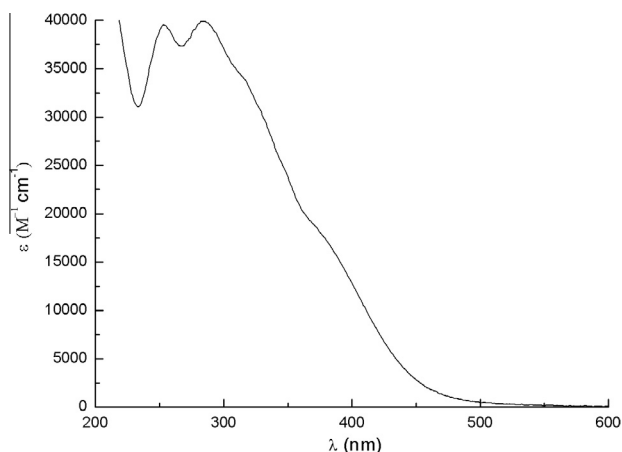
Fig. 1. UV–Vis spectrum of [(CH$_3$CN)(CO)$_3$Re(μ-BBDB)Re(CO)$_3$ (CH$_3$CN)]$^{2+}$, cation of (**3**), in CH$_3$CN at r.t.
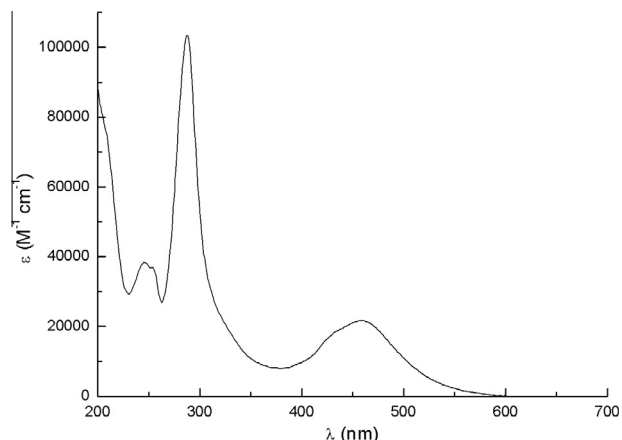
Fig. 2. UV–Vis spectrum of [(bpy)$_2$Ru(μ-BBDB)Ru(bpy)$_2$]$^{4+}$, cation of (**4**), in CH$_3$CN at r.t.

(0.1 M TBAH), at room temperature. Assignments have been made according to previous electrochemical data reported for related complexes [9,21]. E_{pa} values corresponding to Re$^{2+/+}$ couples increase about 0.5 V when changing Cl$^-$ (in **1**) to CH$_3$CN (in **3**), in consistency with the reported spectroscopic changes. On the other hand, redox potential values $E_{1/2} = (E_{pa} + E_{pc})/2$, corresponding to Ru$^{3+/2+}$ couples decrease by almost 0.7 V when changing bpy (in **4**) to NH$_3$ (in **5**), as expected because bipyridyls are strong electron acceptors. The first reduction wave due to the process BBDB$^{0/-}$ appears in all compounds at E_{pc} −1.2 V and is irreversible. In compound (**4**), BBDB is reduced more easily than bpy. No splitting was detected in the oxidative potentials of the dinuclear species

(**3**) and (**4**), indicating a low value of the metal–metal electronic coupling. However, as shown in Fig. 5 complex (**5**) exhibits two oxidative potentials at E_{ox1} = 0.47 V and E_{ox2} = 0.59 V, with a difference of $\Delta E = E_{ox2} - E_{ox1}$ = 0.12 V. The comproportionation constant can be calculated with the equation: $K_c = 10^{\Delta E/0.059}$ [36]. The obtained value is K_c = 100 which is intermediate between the statistical one (K_c = 4) and that detected for a mixed-valent species with a short bridge like 2,2′-bipyrimidine (K_c = 1500) [24]. We deduce that the metal–metal electronic coupling is considerable in (**5**), if we take into account the long distance imposed by the bridging ligand BBDB (~15 Å), a fact that has also been reported in our previous studies with the related ligand 4-PCA [9]. This enhancement of the electronic coupling can be explained by the high degree of delocalization in the bridging ligand, as discussed below in the computational section.

3.6. Photophysical properties

None of the BBDB complexes display luminescense either at r.t. or at 77 K. The fast deactivation process can be attributed to low-lying excited states located at the —C=N—N=C— backbone, as it was confirmed by computational calculations shown below.

3.7. Orbital energies and excited state properties

DFT calculations have recently emerged as powerful tools for predicting molecular properties and reactivity of rhenium and ruthenium compounds. MO calculations of several tricarbonyl-polypyridylrhenium(I) and polypyridyl ruthenium complexes have provided theoretical UV–Vis, emission and IR spectra in good agreement with experimental results [37–58].

In particular, photophysical properties of ruthenium and rhenium complexes can be explained by computational studies. In this work, we have found that neither BBDB nor its complexes are luminescent at room temperature. This abscence can be explained by GAUSSIAN computational calculations, and the results can be correlated with the corresponding properties of the ligands PCA and bpy.

We have already reported the synthesis and physicochemical characterization of a series of compounds of formulae [Re(4,4′-X$_2$-bpy)(CO)$_3$(4-PCA)]$^+$ (with X = Me, H, Ph or CO$_2$Me) [10,11]. Changes in photophysical properties in this series that occur on modifying X have been attributed to an inversion in MO energy levels. In effect, upon adding electron withdrawing substituents to the 2,2′-bipyridine ring; e.g., when going from X = H to X = Ph, the lifetime of the lowest lying triplet excited state ^{3}MLCT increases by 2 orders of magnitude, a result that can be explained by the fact that the emissive Re^{II}(X$_2$bpy)$^-$ excited state lies at a lower energy than the Re^{II}(4-PCA)$^-$ non-emissive excited state in the case of X = Ph, contrary to the case of X = H. This non-emissive state has the LUMO localized in the delocalized π* of the 4-PCA ligand as its main contribution [11].

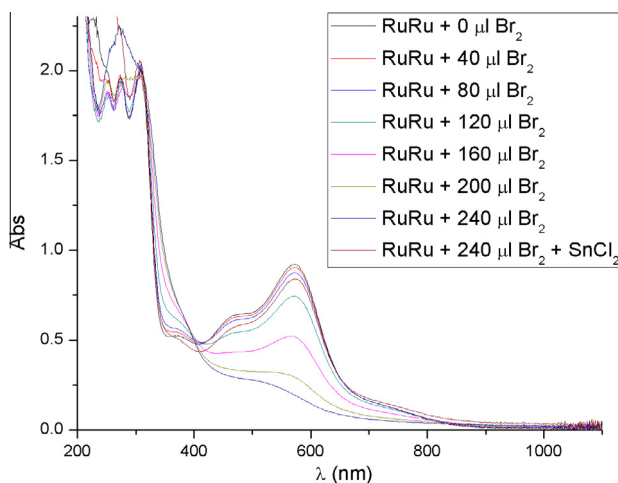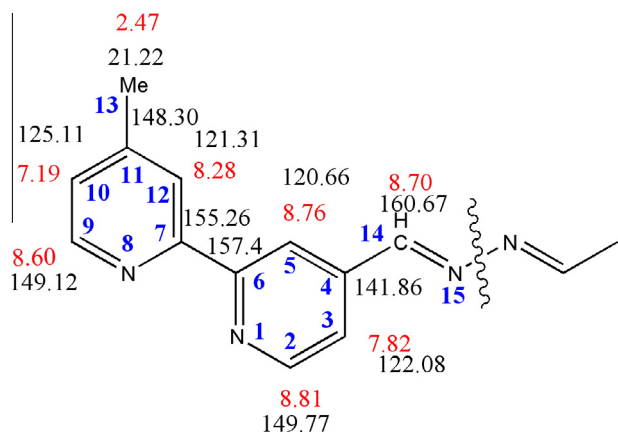**Fig. 3.** Spectrophotometric titration of $[(NH_3)_4Ru(\mu\text{-BBDB})Ru(NH_3)_4]^{4+}$, cation of (**5**), with Br_2 in CH_3CN at r.t.

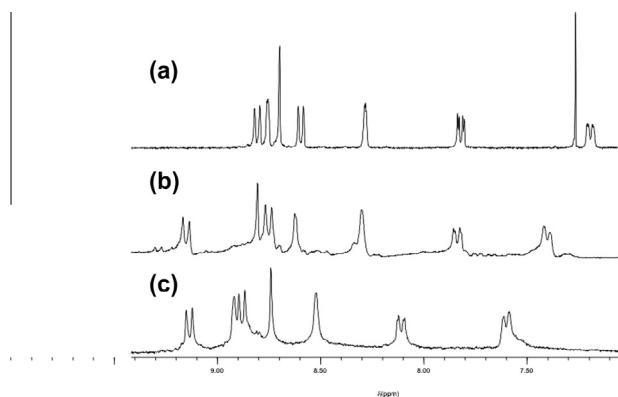**Scheme 4.** Assigments of ^1H NMR data (in red) and ^{13}C NMR data (in black) of BBDB. (Color online.)

Fig. 4. ^1H NMR of: (a) BBDB in $CDCl_3$; (b) $[(NH_3)_4Ru(\mu\text{-BBDB})Ru(NH_3)_4]^{4++}$, cation of (**5**), in CD_3CN, and (c) $[(CH_3CN)(CO)_3Re(\mu\text{-BBDB})Re(CO)_3(CH_3CN)]^{2++}$, cation of (**3**), in CD_3CN.

In this work, in order to acquire a theoretical explanation of these unusual photophysical changes, we have performed DFT calculations of molecular orbitals of the above mentioned complexes using the polarizable continuum model PCM in CH_3CN. Both bpz (2,2′-bipirazine) and 4,4′-CO_2H-bpy have been included as diimine ligands. We have also carried out TD-DFT calculations of electronic transitions of these species in the same solvent.

Fig. 6 shows the electronic density diagrams of some molecular orbitals of $[Re(bpy)(CO)_3(4\text{-PCA})]^+$: it can be clearly envisaged that the HOMO has a major contribution (71%) from the fragment $[Re(CO)_3]$ and some contributions from 4-PCA. The LUMO is located mainly at the 4-PCA ligand (98%) and the LUMO+1 is located mainly at the bpy ligand (91%). The molecular orbitals energies and% contribution of each group for all the series are listed in Supplementary Table S1, for the 5 highest occupied molecular orbitals and the 5 lowest unoccupied molecular orbitals.

In all cases, the LUMO located at 4-PCA is close in energy to the LUMO located at X_2bpy. As it is shown in Fig. 7, where the energies of the MOs have been depicted for all complexes, an inversion is predicted between the two lowest unoccupied MOs, in going from Me_2bpy to bpz in the series $[Re(diimine)(CO)_3(4\text{-PCA})]^+$. While the energy of the LUMO orbital located at 4-PCA is maintained almost constant, the energy of the LUMO orbital located at the diimine decreases with its increasing electron withdrawing abilities. Energy changes at the HOMO d_π orbitals of the rhenium are smaller than those of the LUMO orbital at the diimine. Therefore, the energies of the lowest electronic transitions – considering them approximately as pure HOMO (d_πRe) → LUMO (π^*bpy) – shift to lower values when going from Me_2bpy to bpz, in consistency with our experimental results [11,59]. PDOS (partial density of states), orbital energies and% contribution of each group to each molecular orbital are shown graphically for all complexes in Supplementary Figs. S1–S6. Fig. 7 also shows that in the case of $[Re(bpy)(CO)_3(4,4′\text{-bpy})]^+$ (4,4′-bpy = 4,4′-bipyridine), the three highest occupied molecular orbitals are mainly located at the $[Re(CO)_3]$ group, while the two lowest unoccupied molecular orbitals are located at bpy.
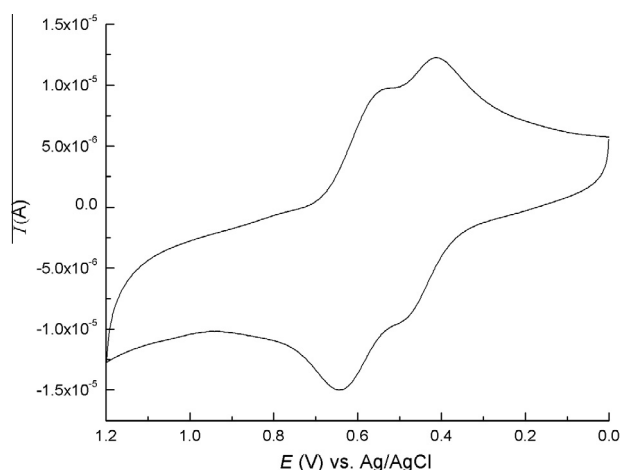
The lowest energy transition can be attributed to MLLCT (metal–ligand to ligand charge transfer) from $[Re(CO)_3]$ group to 4-PCA and X_2bpy. The computed excitation energies for this series of complexes were underestimated, as usually observed when using B3LYP functionals [55] and could not be improved in this work by using other functionals or higher amounts of correlation energies. Vlček et al. [50] have suggested that using PBE1PBE functionals gives better results than B3LYP functionals, but we have obtained very similar qualitative and quantitative information with both functionals in the cases where convergence could be reached. Nevertheless, the trend of the observed UV–Vis spectra is reasonably well explained. In effect, the experimental values of λ_{max} change in the order: Me_2bpy < bpy < Ph_2bpy < $(CO_2Me)_2$bpy < $(CO_2H)_2$bpy < bpz [59], in consistency with the trend predicted by theory.

On the other hand, BBDB is composed of 2,2′-bpy and 4-PCA ligands. As shown in Fig. 8, the LUMO of BBDB is almost completely delocalized over the —C=N—N=C— backbone, as already determined for 4-PCA, indicating that a similar behaviour for both ligands is expected in relation to orbital interactions and intramolecular electron transfers over the bridge in their complexes.

Fig. S7 shows the electronic density diagrams of some molecular orbitals of $[Re(BBDB)(CO)_3Cl]$. It can be clearly envisaged that the HOMO has a major contribution (74%) from the $[Re(CO)_3]$ core and some contributions from Cl (21%) while the LUMO and LUMO+1 are located mainly at the BBDB ligand (96% and 97% respectively). Cl^- is a σ-donor ligand contributing to the electron density at the metal center and so it can be considered as part of the group $[Re(CO)_3Cl]$ [37]. The molecular orbitals energies and % contribution of each group for the series $[Re(L)(CO)_3X]^{n+}$ (with L = bpy, BBDB; X = Cl, CH_3CN, 4-PCA; $n = 0,1$) are shown in Fig. S8. Comparison with the complex $[Re(bpy)(CO)_3Cl]$ shows only a difference in the LUMO's located at lower energy for the BBDB complex. Inclusion of CH_3CN as a sixth ligand instead of Cl^- mix the $[Re(CO)_3]$ contributions with those of BBDB, as was the case with 4-PCA in $[Re(CO)_3(bpy)(4\text{-PCA})]^+$. The orbitals of CH_3CN do not contribute to the electronic absorptions. We deduce that the
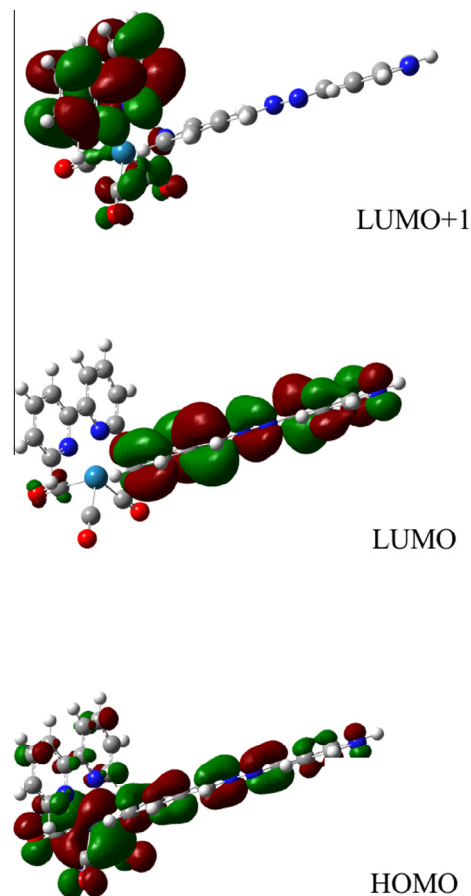
Table 2
Electrochemical data, in CH₃CN, at 22 °C.

Compound	Process	E_{pa} [V][a]	E_{pc} [V][a]
BBDB	BBDB⁰/⁻		−1.26
[Re(BBDB)(CO)₃(Cl)], (**1**)	Re²⁺/⁺	1.42	
	BBDB⁰/⁻	−1.25	−1.33
	Re⁺/⁰	−1.37	−1.47
	BBDB⁻/²⁻		−1.64
	BBDB²⁻/³⁻		−1.90
[(CH₃CN)(CO)₃Re(μ-BBDB)Re(CO)₃(CH₃CN)]²⁺, cation of (**3**)	Re²⁺/⁺	1.89	
	BBDB⁰/⁻		−1.30
	Re⁺/⁰	−1.42	−1.54
[(bpy)₂Ru(μ-BBDB)Ru(bpy)₂]⁴⁺, cation of (**4**)	Ru³⁺/²⁺	1.34	1.26
	BBDB⁰/⁻		−1.22
	bpy⁰/⁻	−1.30	−1.42
	bpy⁻/²⁻	−1.48	−1.62
	bpy²⁻/³⁻	−1.74	−1.86
[(NH₃)₄Ru(μ-BBDB)Ru(NH₃)₄]⁴⁺, cation of (**5**)	Ru³⁺/²⁺	0.65	0.53
	Ru³⁺/²⁺	0.51	0.43
	BBDB⁰/⁻		−1.54
	BBDB⁻/²⁻		−1.91
[(Ru(4-Me-4′-CO₂H-bpy)(bpy)₂]²⁺, cation of (**6**)	Ru³⁺/²⁺	1.38	1.26
	bpy⁰/⁻	−1.31	−1.41
	bpy⁻/²⁻	−1.50	−1.62
	bpy²⁻/³⁻	−1.74	−1.86
[Ru (4-Me-4′-CO₂H-bpy)(CN)₄]²⁻, anion of (**7**)	Ru³⁺/²⁺	0.45	0.37

[a] vs. Ag/AgCl.

Fig. 5. Cyclic voltammogram of [(NH₃)₄Ru(μ-BBDB)Ru(NH₃)₄]⁴⁺, cation of (**5**), in CH₃CN, TBAH 0.1 M, at 100 mV/s.

Fig. 6. Electronic density diagrams of some molecular orbitals of [Re(bpy)(CO)₃(4-PCA)]⁺.

lowest-lying transitions are not purely MLCT, but also include IL (4-PCA or BBDB) contributions. For complexes with BBDB, the aza-butadiene bridge decreases the energy of the LUMO's and increases the energies of the HOMO's located in the ligand, resulting in the LUMO in all complexes being delocalized over BBDB. In this way, it explains their lack of emission, considering the fast non-radiative decays expected for excited states involving ligands with a —C=N—N=C— backbone, such as 4-PCA [9]. In consistency with this prediction, [Re(bpy)(CO)₃(4,4′-bpy)]⁺ emits at r.t. because the LUMO located at 4,4′-bpy is much higher in energy than that located at bpy. However, on protonation of 4,4′-bpy in aqueous solution, the energy of its LUMO becomes lower than that of bpy and consequently emission is almost completely quenched [12].

A spin density plot of the complex [Re(BBDB)(CO)₃(CH₃CN)]⁺ used as model for complex (**3**) shows the same trend: the spin density is localized in the ligand BBDB and the complex is still non-emissive. This result suggests that all Re complexes that include BBDB such as (**1**) and (**3**) will not emit, considering the fast decays of the excited states involving this ligand. Calculations indicate that luminescence could be recovered by introducing a modified bpy ligand with lower LUMO energies than BBDB or otherwise by photoisomerization or reduction of the azo functionality [60].
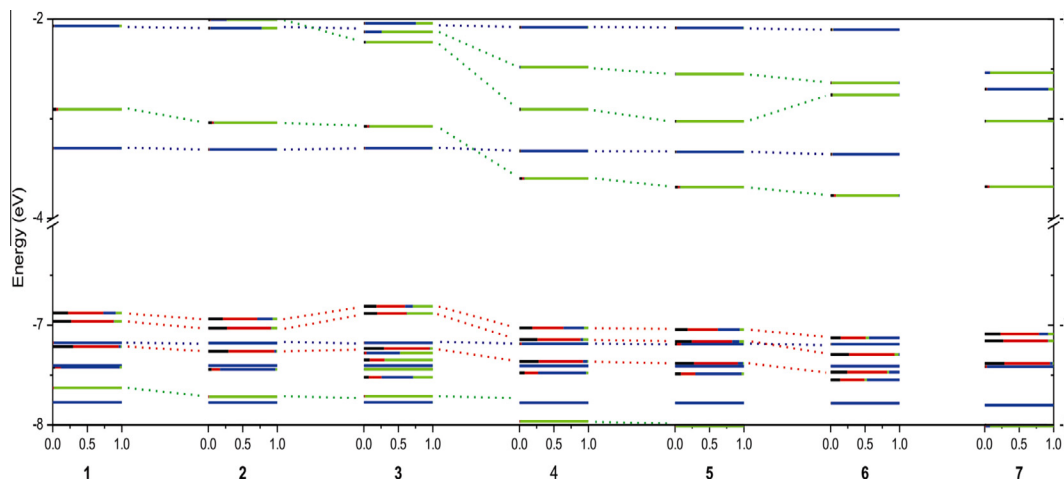
Fig. 7. Molecular orbital diagrams of complexes: **1** = [Re(Me₂bpy)(CO)₃(4-PCA)]⁺, **2** = [Re(bpy)(CO)₃(4-PCA)]⁺, **3** = [Re(Ph₂bpy)(CO)₃(4-PCA)]⁺, **4** = [Re((CO₂Me)₂bpy)(CO)₃(4-PCA)]⁺, **5** = [Re((CO₂H)₂bpy)(CO)₃(4-PCA)]⁺, **6** = [Re(bpz)(CO)₃(4-PCA)]⁺ and **7** = [Re(bpy)(CO)₃(4,4′-bpy)]⁺, calculated at the DFT/B3LYP/LANL2DZ/CPCM acetonitrile level of theory. The colours indicate % contribution of: CO's (black), Re (red), 4-PCA or 4,4′-bpy (blue), 4,4′-X₂-bpy or bpz (red). (Color online.)
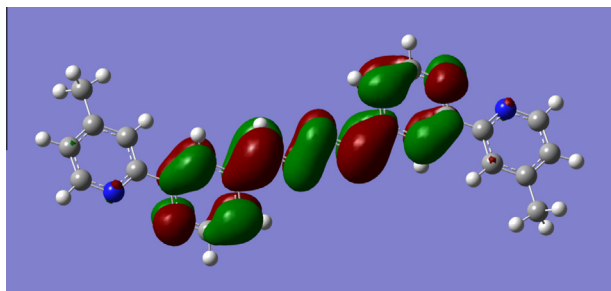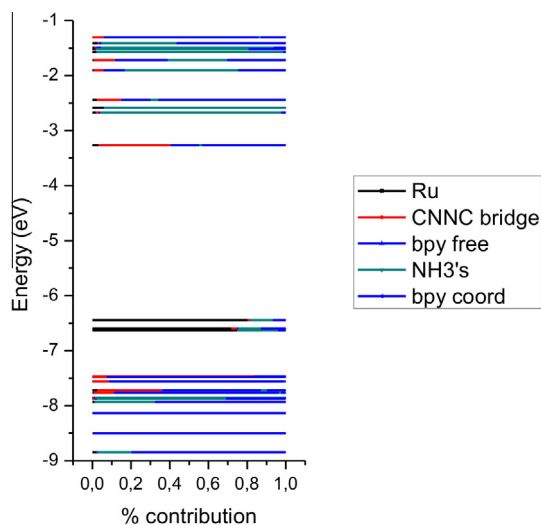

Fig. 8. LUMO of BBDB.

Fig. 9. MO energy diagram for the dinuclear ruthenium complex [(NH₃)₄Ru(μ-BBDB)Ru(NH₃)₄]⁴⁺, cation of (**5**).

Molecular orbital diagrams with Mulliken population analysis were determined by using DFT methods for ruthenium complexes (**4**) and (**5**). In (**4**), the LUMO located at BBDB is lower in energy than that located in bpy, in agreement with the higher E_{pc} value of the BBDB$^{0/-}$ couple compared to that of bpy$^{0/-}$ (see Table 2) and with its lack of luminescence. The calculated electronic coupling in (**4**) was lower than that in (**5**) in accord to experimental

results: no splitting of the voltammetric oxidative waves of (**4**) was detected in contrast to the observed 0.12 V splitting in (**5**). A molecular orbital energy diagram of the cation of complex (**5**) is depicted in Fig. 9. Inclusion of free bpy ligands in (**4**) stabilize the d$_\pi$ Ru HOMO's; an increased energy of the lowest-lying MLCT transition is thus predicted for (**4**) as compared to (**5**), a result confirmed by UV–Vis measurements (see Table 1).

In conclusion, the computational studies are consistent with the electrochemical and spectroscopic data obtained for the complexes described in this work. The excited state behaviour depends on the LUMO orbital centered at the BBDB ligand, which shows a remarkable similarity with 4-PCA, where the LUMO is delocalized over the —C≡N—N≡C— backbone [10,11].

4. Conclusions

A new bridging ligand (BBDB) useful for building novel coordination compounds, has been synthetized and characterized by analytical, spectroscopic and electrochemical techniques. Synthesis of novel coordination compounds of tricarbonylrhenium(I), polypyridylruthenium(II) and amamineruthenium(II) moieties containing BBDB were carried out and hydrolysis products with ruthenium bipyridyls and cyanides were characterized. The determined comproportionation constant K_c for the dinuclear BBDB mixed-valent complex with ruthenium ammines indicates a considerable coupling for the imposed metal-metal distance. Spectroscopic results for these complexes were compared with DFT calculations and rationalized with a previous series including the related ligand 4-PCA. Lack of luminescence of all complexes is explained by the fast non-radiative decay from the LUMO orbital mainly localized at the delocalized bridging unit with the aza-butadiene linker. Luminescence could be recovered either by introducing modified bpy ligands or by photoisomerization or reduction of the azo functionality. Moreover, the contribution of different fragment in the molecule to every MO could be assessed by using Mulliken population analysis.

Members of the Research Career from CONICET, Argentina. We thank Mr. Fabian Ehret and Dr. Wolfgang Kaim (Suttgart University, Germany) for help in spectrophotometric measurements of mixed-valent species.

Appendix A. Supplementary data

Supplementary (Energies and % contributions of 5 highest molecular orbitals and 5 lowest molecular orbitals for 4-PCA complexes, PDOS spectra, orbital energies and % contribution of each group for 4-PCA complexes, spin density pictures and MO diagrams for Re complexes.) data associated with this article can be found, in the online version, at http://dx.doi.org/10.1016/j.poly.2013.12.018.

References

[1] A. Juris, V. Balzani, F. Barigelletti, S. Campagna, P. Belser, A. Von Zelewsky, Coord. Chem. Rev. 84 (1988) 85.
[2] A.P. Smith, C.L. Fraser, in: J.A. McCleverty, T.J. Meyer, A.B.P. Lever (Eds.), Comprehensive Coordination Chemistry II, vol. 1, Elsevier Ltd., 2003, p. 1 (Chapter 1.1).
[3] F. Fagalde, N.E. Katz, Polyhedron 14 (1995) 1213.
[4] M. Glöckle, W. Kaim, N.E. Katz, M.E. García, J. Fiedler, Inorg. Chem. 38 (1999) 3270.
[5] J.-P. Launay, Chem. Soc. Rev. 30 (2001) 386.
[6] F. Fagalde, M.E. García, Polyhedron 26 (2007) 17.
[7] R.A. Marcus, N. Sutin, Biochim. Biophys. Acta 811 (1985) 265.
[8] V. Balzani, A. Juris, M. Venturi, Chem. Rev. 96 (1996) 759.
[9] M. Cattaneo, F. Fagalde, N.E. Katz, A.M. Leiva, R. Schmehl, Inorg. Chem. 45 (2006) 127.
[10] M. Cattaneo, F. Fagalde, N.E. Katz, Inorg. Chem. 45 (2006) 6884.
[11] M. Cattaneo, F. Fagalde, N.E. Katz, C.D. Borsarelli, T. Parella, Eur. J. Inorg. Chem. (2007) 5323.
[12] M. Cattaneo, F. Fagalde, C.D. Borsarelli, N.E. Katz, Inorg. Chem. 48 (2009) 3012.
[13] G. Pourrieux, F. Fagalde, I. Romero, X. Fontrodona, T. Parella, N.E. Katz, Inorg. Chem. 49 (2010) 4084.
[14] A.J. Amoroso, M.P. Coogan, J.E. Dunne, V. Fernández-Moreira, J.B. Hess, A.J. Hayes, D. Lloyd, C. Millet, S.J.A. Pope, C. Williams, Chem. Commun. (2007) 3066.
[15] V.W.-W. Yam, C.-C. Ko, N. Zhu, J. Am. Chem. Soc. 126 (2004) 12734.
[16] H. Takeda, O. Ishitani, Coord. Chem. Rev. 254 (2010) 346.
[17] J.H. Alstrum-Acevedo, M.K. Brennaman, T.J. Meyer, Inorg. Chem. 44 (2005) 6802.
[18] W. Kaim, A. Klein, M. Glöckle, Acc. Chem. Res. 33 (2000) 763.
[19] T.L. Easun, W.Z. Alsindi, N. Deppermann, M. Towrie, K.L. Ronayne, X.-Z. Sun, M.D. Ward, M.W. George, Inorg. Chem. 48 (2009) 8759.
[20] G.F. Strouse, J.R. Schoonover, R. Duesing, S. Boyde, W.E. Jones Jr., T.J. Meyer, Inorg. Chem. 34 (1995) 473.
[21] S. Van Wallendael, R.J. Shaver, D.P. Rillema, B.J. Yoblinski, M. Stathis, T.F. Guarr, Inorg. Chem. 29 (1990) 1761.
[22] J.A. Baiano, D.L. Carlson, G.M. Wolosh, D.E. DeJesus, C.F. Knowles, E.G. Szabo, W.R. Murphy Jr., Inorg. Chem. 29 (1990) 2327.
[23] M.G. Mellace, F. Fagalde, N.E. Katz, I.G. Crivelli, A. Delgadillo, A.M. Leiva, B. Loeb, M.T. Garland, R. Baggio, Inorg. Chem. 43 (2004) 100.
[24] R.R. Ruminski, J.D. Petersen, Inorg. Chem. 21 (1982) 3706.
[25] R.R. Ruminski, T. Cockroft, M. Shoup, Inorg. Chem. 27 (1988) 4026.
[26] J.E.B. Johnson, C. de Groff, R.R. Ruminski, Inorg. Chim. Acta 187 (1991) 73.
[27] J.E. Sutton, H. Taube, Inorg. Chem. 20 (1981) 3125.
[28] N. Nickita, M.J. Belousoff, A.I. Bhatt, A.M. Bond, G.B. Deacon, G. Gasser, L. Spiccia, Inorg. Chem. 46 (2007) 8638.
[29] J.-M. Herrera, S.G. Baca, H. Adams, M.D. Ward, Polyhedron 25 (2006) 869.
[30] M.J. Frisch, et al., GAUSSIAN-03, revision C.02; Gaussian Inc., Wallinford, CT, 2004.
[31] J.P. Perdew, K. Burke, M. Ernzerhof, Phys. Rev. Lett. 77 (1996) 3865.
[32] C. Adamo, V. Barone, J. Chem. Phys. 110 (1999) 6158.
[33] N.M. O'Boyle, A.L. Tenderholt, K.M. Langner, J. Comput. Chem. 29 (2008) 839. Available from: http://gausssum.sf.net.
[34] L.A. Worl, R. Duesing, P. Chen, L. Della, Dalton Trans. (1991) 849.
[35] M.E. García Posse, F. Fagalde, M.M. Vergara, N.E. Katz, Polyhedron 17 (1998) 2733.
[36] M. Vergara, M.E. García Posse, F. Fagalde, N.E. Katz, J. Fiedler, B. Sarkar, M. Sieger, W. Kaim, Inorg. Chim. Acta 363 (2010) 163.
[37] D.M. Dattelbaum, K.M. Omberg, J.R. Schoonover, R.L. Martin, T.J. Meyer, Inorg. Chem. 41 (2002) 6071.
[38] L. Yang, A.-M. Ren, J.-K. Feng, X.-D. Liu, Y.-G. Ma, H.-X. Zhang, Inorg. Chem. 43 (2004) 5961.
[39] D.M. Dattelbaum, R.L. Martin, J.R. Schoonover, T.J. Meyer, J. Phys. Chem. A 108 (2004) 3518.
[40] D.M. Dattelbaum, K.M. Omberg, P.J. Hay, N.L. Gebhart, R.L. Martin, J.R. Schoonover, T.J. Meyer, J. Phys. Chem. A 108 (2004) 3527.
[41] L. Yang, A.-M. Ren, J.-K. Feng, X.-J. Liu, Y.-G. Ma, M. Zhang, X.-D. Liu, J.-C. Shen, H.-X. Zhang, J. Phys. Chem. A 108 (2004) 6797.
[42] J.M. Villegas, S.R. Stoyanov, W. Huang, D.P. Rillema, Inorg. Chem. 44 (2005) 2297.
[43] A.M. Blanco Rodríguez, A. Gabrielsson, M. Motevalli, P. Matousek, M. Towrie, J. Sebera, S. Záliš, A. Vlček Jr, J. Phys. Chem. A 109 (2005) 5016.
[44] W.R. Browne, N.M. O'Boyle, J.J. McGarvey, J.G. Vos, Chem. Soc. Rev. 34 (2005) 641.
[45] A. Gabrielsson, M. Busby, P. Matousek, M. Towrie, E. Hevia, L. Cuesta, J. Perez, S. Záliš, A. Vlček Jr., Inorg. Chem. 45 (2006) 9789.
[46] D. Rappoport, F. Furche, Lect. Notes Phys. 706 (2006) 337.
[47] A. Albertino, C. Garino, S. Ghiani, R. Gobetto, C. Nervi, L. Salassa, E. Rosenberg, A. Sharmin, G. Viscardi, R. Buscaino, G. Croce, M. Milanesio, J. Organomet. Chem. 692 (2007) 1377.
[48] R. Kirgan, M. Simpson, C. Moore, J. Day, L. Bui, C. Tanner, D.P. Rillema, Inorg. Chem. 46 (2007) 6464.
[49] B. Machura, R. Kruszynski, Polyhedron 26 (2007) 3336.
[50] A.J. Vlček Jr., S. Záliš, Coord. Chem. Rev. 251 (2007) 258.
[51] G.-J. Zhao, X. Zhou, T. Liu, Q.-C. Zheng, F.-Q. Bai, J. Mol. Struct. 855 (2008) 52.
[52] Y. Gao, S. Sun, K. Han, Spectrochim. Acta, Part A 71 (2009) 2016.
[53] A. Vlček Jr., Top. Organomet. Chem. 29 (2010) 73.
[54] B. Machura, A. Świtlicka, I. Nawrot, K. Michalik, Chem. Commun. 13 (2010) 1317.
[55] B. Machura, M. Wolff, M. Jaworska, P. Lodowski, E. Benoist, C. Carrayon, N. Saffon, R. Kruszynski, Z. Mazurak, J. Organomet. Chem. 696 (2011) 3068.
[56] B. Machura, M. Wolff, I. Gryca, A. Palion, K. Michalik, Polyhedron 30 (2011) 2275.
[57] M. Sánchez-Lozano, E.M. Vázquez-López, J.M. Hermida-Ramón, C.M. Estévez, Polyhedron 30 (2011) 953.
[58] R. Baková, M. Chergui, C. Daniel, A. Vlček Jr., S. Záliš, Coord. Chem. Rev. 255 (2011) 975.
[59] M. Cattaneo, PhD dissertation, Universidad Nacional de Tucumán, Argentina, 2008.
[60] J. Otsuki, N. Omokawa, K. Yoshiba, I. Yoshikawa, T. Akasaka, T. Suenobu, T. Takido, K. Araki, S. Fukuzumi, Inorg. Chem. 42 (2003) 3057.